Lattice Boltzmann Study of Hydrodynamic Spinodal Decomposition

W. R. Osborn, E. Orlandini, Michael R. Swift, J. M. Yeomans, and Jayanth R. Banavar*
Theoretical Physics, Oxford University, 1 Keble Road, Oxford OX1 3NP, United Kingdom
(Received 8 August 1995)

We study both the dynamics of dissolution of an equilibrium interface and phase separation in two-dimensional fluids using lattice Boltzmann simulations. Results for a liquid-gas system and a binary fluid are compared. For symmetric quenches in the liquid-gas system, single-phase domains grow like t^{α}, where $\alpha = 1/2$ for high viscosities (corresponding to early times), crossing over to $\alpha = 2/3$ for low viscosities (later times). For a binary fluid the crossover is between $\alpha = 1/3$ and $\alpha = 2/3$. This behavior is compared to that for nonsymmetric quenches.

PACS numbers: 47.20.Hw, 05.70.Ln, 64.60.Qb

When a system is quenched into the two-phase region, phase separation occurs through the formation and subsequent growth of single-phase domains. Once the domains are established there is strong evidence that the system evolves with time t in a way that is scale invariant. Hence lengths such as the domain size grow according to a power law $L \sim t^{\alpha}$. The values of the exponent α are well understood in binary alloys and magnetic systems where the growth is driven by the surface tension: for a nonconserved order parameter, model A, $\alpha = 1/2$ and for a conserved order parameter, model B, $\alpha = 1/3$ [1]. However, in fluids, where hydrodynamic modes can facilitate phase separation, the situation is far from clear.

In this Letter we describe lattice Boltzmann simulations of interface dissolution and of phase separation in a two-dimensional fluid. Our results qualitatively extend those that have appeared previously in the literature in that we are able to treat *both* a liquid-gas system *and* a binary fluid within the same framework. Moreover, we are able to adjust the fluid viscosity, or equivalently change the time scale of the simulations and see the crossover between the scaling behavior at short times, which is driven by surface tension and diffusion and that for long times, which is a result of hydrodynamic flow. We find that in a symmetric quench for a liquid-gas system $\alpha = 1/2$ for high viscosities (short times) and $2/3$ for low viscosities (long times), whereas for a binary fluid the crossover is between $\alpha = 1/3$ and $2/3$. The value $2/3$ is the result of the interplay between the inertia of the fluid and the surface driving force [2]. Deviations from these values in an off-symmetric quench of a binary fluid may be due to a slow crossover regime [3].

Numerical approaches to the simulation of phase separation in two-dimensional fluids have included molecular-dynamics and numerical integration of the Ginzburg-Landau equations. There are many conflicting results. Molecular dynamics simulations have the advantage of being faithful to the microscopic nature of the fluid. However, as a result, they are computationally very demanding. Surprisingly, values of α close to $1/2$ and $1/3$ have been obtained for a symmetric and off-symmetric quench, respectively, in a binary fluid system [4]. Although $\alpha = 2/3$ was reported for later times, this was subsequently explained as a result of incomplete averaging [5]. Simulations for a liquid-gas system obtained $\alpha = 1/2$ [6]. A recent paper reported effective values of α which varied from 0.1 to 0.5 for both binary and one-component fluids [7]. Therefore there is still no consensus on the physics of the early time regime and no evidence that molecular dynamics simulations are at present capable of accessing hydrodynamic growth.

In the time-dependent Landau-Ginzburg approach the fluid is modeled by a set of coupled Langevin equations for the order parameter and fluid momentum. Thus the microscopic behavior is severely abstracted; in particular, the fluid no longer explicitly obeys the Navier-Stokes equations and the density-momentum coupling is introduced phenomenologically. The advantage of this method is that it is possible to access longer time scales than molecular dynamics. Early work by Farrell and Valls [8] gave $\alpha \sim 0.3$ for short times and $\alpha = 0.65 \pm 0.03$ for long times in symmetric quenches. Results for off-symmetric quenches were inconclusive [9]. Later results [10] have suggested that α depends on the strength of the fluid order-parameter coupling and that the long time behavior for off-symmetric quenches corresponds to $\alpha \sim 0.46$.

The lattice Boltzmann approach provides an alternative numerical technique which is ideally suited to investigate phenomena on a hydrodynamic length scale. Microscopic interactions are not explicitly defined, but the fluid flows according to the Navier-Stokes equations with motion governed by viscosities that can easily be varied.

Previous simulations obtained $\alpha = 0.66$ for a symmetric quench [11] and $\alpha = 1/3$ crossing over to $\alpha = 0.4 \pm 0.03$ for an off-symmetric quench [12]. These simulations, restricted to binary fluids at a single viscosity, were based on the immiscible fluid model of Gunstensen *et al.* [13]. In this approach interfaces are introduced phenomenologically by changes in the collision rules. One consequence is that the correct dynamics cannot hold for $T \geq T_c$, a feature which may be important at very early times [3]. In the lattice Boltzmann simulations reported here, phase separation is imposed by demanding that the pressure tensor and diffusivity take the correct

0031-9007/95/75(22)/4031(4)$06.00

form [14,15], leading to equilibrium densities and interface profiles that correspond to an input equation of state.

Lattice Boltzmann simulations are set up by defining a probability distribution $f_i(\vec{x},t)$ at each lattice site $\vec{x}$, where i denotes a lattice direction (corresponding to a unit vector $\vec{e}_i$) or a zero velocity state. Physical quantities, for example, the density n and the macroscopic velocity $\vec{u}$, are related to the f_i through

$$n = \sum_i f_i, \quad n\vec{u} = \sum_i f_i \vec{e}_i . \tag{1}$$

The probability distribution evolves in two steps. Firstly the partial densities move to the neighboring site along $\vec{e}_i$ with speed c. They then relax to equilibrium via a single relaxation time τ [16]

$$f_i(\vec{x} + c\vec{e}_i, t + \Delta t) - f_i(\vec{x},t) = -\frac{1}{\tau}(f_i - f_i^0), \tag{2}$$

where the equilibrium distribution

$$\begin{aligned} f_i^0 &= A + Be_{i\alpha}u_\alpha + Cu^2 + Du_\alpha u_\beta e_{i\alpha}e_{i\beta} \\ &\quad + F_\alpha e_{i\alpha} + G_{\alpha\beta}e_{i\alpha}e_{i\beta}, \\ f_0^0 &= A_0 + C_0 u^2. \end{aligned} \tag{3}$$

The coefficients in (3) contain the physics of the problem. Our aim here is to capture the nonideal behavior of a simple fluid, or the immiscibility of a binary mixture. To do this we allow these coefficients to be functions of density gradients as well as the density defined locally at each site. They can then be chosen to ensure that the dynamics is described by the Navier-Stokes equations for a compressible fluid with a nonideal pressure tensor and that the density relaxes to an equilibrium defined by an input free energy.

For a single component nonideal fluid [14] this is done by demanding that the first three moments of f_i^0 take the form

$$\sum_i f_i^0 = n, \quad \sum_i f_i^0 \vec{e}_i = n\vec{u}, \tag{4}$$

$$\sum_i f_i^0 e_{i\alpha}e_{i\beta} = nu_\alpha u_\beta + P_{\alpha\beta} - \lambda u_\gamma \partial_\gamma n \delta_{\alpha\beta}. \tag{5}$$

The first two constraints correspond to local conservation of mass and momentum. The third constraint, in which $P_{\alpha\beta}$ is the pressure tensor of the nonideal fluid, ensures that the fluid reaches a nonuniform equilibrium state consistent with thermodynamics, as defined in the usual way by a free energy [17]. The term in λ, the shear viscosity, is included in this expression to partially restore Galilean invariance of the flow in regions of high density gradients.

For a binary liquid mixture [15] the major new feature in the lattice Boltzmann approach is the necessity for two distribution functions f_i and g_i corresponding to the sum n and difference Δn of the two fluid densities

$$n = \sum_i f_i, \quad \Delta n = \sum_i g_i . \tag{6}$$

The mean fluid velocity is then defined by

$$n\vec{u} = \sum_i f_i \vec{e}_i . \tag{7}$$

Both f_i and g_i evolve according to Eq. (2) with equilibrium distributions defined as in Eq. (3). We choose the coefficients in these equilibrium distribution functions to ensure that the total density obeys the Navier-Stokes equations with a nonideal pressure tensor, that the density difference evolves according to a convective diffusion equation driven by chemical potential gradients, and that the equilibrium state corresponds to an input free energy. This is again achieved by forcing the first three moments of f_i^0 to be given by Eqs. (4) and those of g_i^0 to obey

$$\sum_i g_i^0 = \Delta n, \quad \sum_i g_i^0 \vec{e}_i = \Delta n \vec{u}, \tag{8}$$

$$\sum_i g_i^0 e_{i\alpha}e_{i\beta} = \Gamma \Delta\mu \delta_{\alpha\beta} + \Delta n u_\alpha u_\beta . \tag{9}$$

Here $\Delta\mu$ is the chemical potential difference between the two components and Γ is the mobility.

For the single component model we choose to simulate a van der Waals fluid corresponding to the free energy density

$$\psi(\vec{r}) = \frac{\kappa}{2} |\nabla n(\vec{r})|^2 + nT \ln\left(\frac{n}{1-nb}\right) - an^2, \tag{10}$$

whereas for the two-component system we work with the simplest model of a binary fluid: two ideal gases with a mutual interaction described by the free energy density

$$\begin{aligned} \psi(\Delta n, n, T) &= \frac{\lambda}{4} n\left(1 - \frac{\Delta n^2}{n^2}\right) - Tn \\ &\quad + \frac{T}{2}(n + \Delta n)\ln\left(\frac{n+\Delta n}{2}\right) + \frac{T}{2}(n - \Delta n) \\ &\quad \times \ln\left(\frac{n-\Delta n}{2}\right) + \frac{\kappa}{2}|\nabla(n)|^2 + \frac{\kappa}{2}|\nabla(\Delta n)|^2. \end{aligned} \tag{11}$$

$P_{\alpha\beta}$ and $\Delta\mu$ can be determined from the free energies [17]. The explicit forms of the continuum equations simulated by this approach are given in Refs. [14,15].

As a test of the dynamics inherent in the these models, and in order to elucidate the universality classes of the two different schemes, we first present results for interface dissolution. An equilibrium interface was set up for $T < T_c$ and the decay of a nonequilibrium surface tension $\sigma \propto \int(\partial\phi/\partial z)^2 dz$, where ϕ is the order parameter (n for the one-component and Δn for the binary fluid), was measured following an instantaneous change of temperature. The time dependence of σ was seen to depend on whether the final temperature T_f was above or equal to the critical temperature T_c. The results are shown in Fig. 1. For the liquid-gas system

$$\sigma \sim t^{-3/2}, \quad T_f = T_c, \quad \sigma \sim e^{-t}, \quad T_f > T_c, \tag{12}$$

whereas for the binary fluid

$$\sigma \sim t^{-1/4}, \quad T_f = T_c, \quad \sigma \sim t^{-1/2}, \quad T_f > T_c. \tag{13}$$

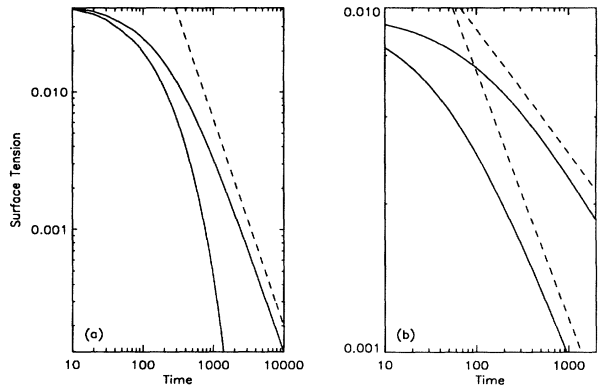

FIG. 1. Decay of the surface tension σ for (a) a liquid gas system and (b) a binary fluid following an instantaneous change of temperature from $T < T_c$ to $T = T_c$ (right hand curve) and $T > T_c$. The dashed lines have the slopes given in the text.

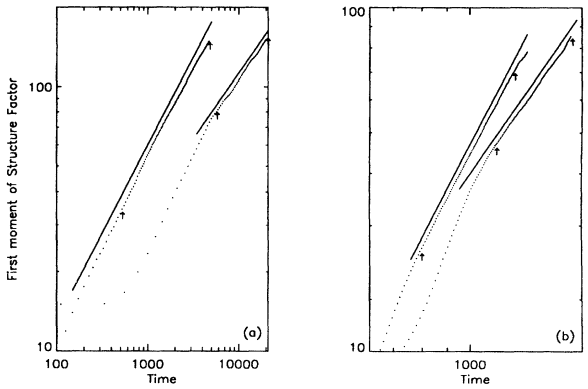

FIG. 2. Variation of length scale with time for (a) symmetric and (b) off-symmetric quenches of a liquid-gas system. Results on the right are for the high viscosity. The solid lines which have slopes 1/2 and 2/3 are included as a guide to the eye.

These results, which are in agreement with the predictions of Ma *et al.* [18], can be understood in terms of simple scaling arguments. Note that $\sigma \sim \phi_0^2/L$, where L is the interface width and ϕ_0 is the value of the order parameter far from the interface. For model B $L \sim t^{1/4}$ at $T = T_c$, $L \sim t^{1/2}$ at $T > T_c$, and ϕ_0 remains constant leading to the results in Eq. (13). For model A $L \sim t^{1/2}$ for $T \geq T_c$. Although ϕ_0 is constant for very early times, this regime is inaccessible to the simulations, and the results in Eq. (12) correspond to later times when $\phi_0 \sim t^{-1/2}$, $T = T_c$ and $\phi_0 \sim e^{-t}$, $T > T_c$.

These results clearly indicate that the two lattice Boltzmann schemes follow model A (liquid-vapor) and model B (binary mixture) dynamics, respectively, in the regime where hydrodynamics is unimportant. These results also demonstrate that our lattice Boltzmann approach captures the correct dynamics in the one-phase region above T_c and at the critical temperature itself, a feature not present in other lattice Boltzmann schemes.

We now describe results for domain growth. For the van der Waals fluid the simulations were performed with $a = 9/49$ and $b = 2/21$ giving a critical temperature $T_c = 0.571$. All quenches were to $T = 0.55$ where the coexisting densities are $n = 4.91$ and $n = 2.22$. Each simulation was started with small fluctuations in the density about a mean value $\bar{n}$ that was either symmetric ($\bar{n} = 3.5$) or off symmetric ($\bar{n} = 3.0$). Results were obtained for lattices of sizes up to 1024×1024. For the binary fluid the simulations were performed with $n = 1$ and $\lambda = 1.1$ corresponding to $T_c = 0.55$. All quenches were to $T = 0.51$ where the coexisting density differences are $\Delta n = \pm 0.45$. The symmetric quench corresponds to initial conditions with mean $\overline{\Delta n} = 0$; the off-symmetric quench to $\overline{\Delta n} = 0.14$. Simulations were carried out on lattices of size 256×256.

The viscosity of the fluid was varied by changing τ. The length and time scales were determined by the values of κ and c, respectively. Values of κ were chosen to give an interface of thickness ~ 10 lattice spacings. This provided the best compromise between avoiding the effects of lattice anisotropy and numerical instabilities, while minimizing finite-size effects. c was chosen as small as possible in order to reduce run time while retaining numerical stability. The results are displayed on a scale corresponding to $\Delta t = 1$.

The crossover time between growth driven by the surface tension and hydrodynamic growth increases with increasing viscosity. Therefore we accessed the different regimes by varying the viscosity rather than attempting to study time scales very close to the limits imposed by system size and numerical capacity. The structure factor was checked to obey a scaling form and the length scale of the domains was calculated from its first moment. Typical results are displayed for a liquid-gas system for symmetric and off-symmetric quenches in Figs. 2(a) and 2(b), respectively. Results for a binary fluid are shown in Fig. 3. In each case data are displayed for a high and a

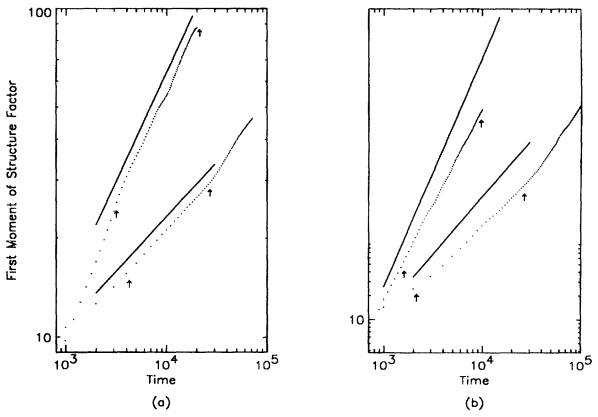

FIG. 3. Variation of length scale with time for (a) symmetric and (b) off-symmetric quenches of a binary fluid. The results on the right are for the high viscosity. The solid lines, which have slopes 1/3 and 2/3 are included as a guide to the eye. Note that the high viscosity results show a crossover to the hydrodynamic regime with increasing time.

TABLE I. Growth exponents α for high and low values of the reduced viscosity $\nu/\sqrt{\sigma}$. Γ is the mobility.

	Symmetric quench			Off-symmetric quench		
	$\nu/\sqrt{\sigma}$		α	$\nu/\sqrt{\sigma}$		α
Liquid	5.63		0.50 ± 0.05	0.8		0.49 ± 0.02
Gas	0.100		0.65 ± 0.03	0.100		0.66 ± 0.01
	$\nu/\sqrt{\sigma}$	Γ	α	$\nu/\sqrt{\sigma}$	Γ	α
Binary	2.77	0.05	0.338 ± 0.009	2.77	0.05	0.28 ± 0.02
Fluid	0.720	0.01	0.66 ± 0.04	0.025	0.01	0.56 ± 0.03

low value of the viscosity chosen to correspond to diffusive and hydrodynamic behavior, respectively. We have also obtained results for intermediate viscosities where a crossover between the two values is apparent. The values of the reduced viscosity, the mobility, and the numerical estimates for α which follow from the simulations are displayed in Table I. The error estimates follow from averaging the slopes in the scaling regime over three to five runs. The spatial averaging inherent in the approach ensured that sample to sample fluctuations were not unacceptably large.

For symmetric quenches our results are consistent with the following conclusions: (i) In the surface-tension driven regime $\alpha = 1/2$ for the liquid-gas system and $1/3$ for the binary fluid. (ii) In the hydrodynamic regime $\alpha = 2/3$ for both models. For off-symmetric quenches the exponents are the same for the liquid-gas system but substantially lower for the binary fluid.

A possible explanation of the results for off-symmetric quenches is provided by the work of Corberi, Coniglio, and Zannetti [3]. These authors suggest that there is a crossover between a very early scaling regime, where the growth is diffusive, and characterized by a trivial fixed point with exponents corresponding to those obtained for the growth of the interfacial width at T_c, and a nontrivial fixed point corresponding to phase ordering. The crossover occurs for later times as the asymmetry of the quench becomes greater. It seems plausible that in the off-symmetric quenches reported here, the system is still in the crossover regime. This is apparent for the binary fluid (in agreement with previous simulations [10,12]) but not for the liquid-gas system where the exponents of the two fixed points are equal.

Another avenue that remains to be explored fully is the effect of thermal fluctuations on the early time scaling behavior. It has been suggested that these are relevant in two dimensions [1] when hydrodynamic transport is operative. However, recent lattice Boltzmann simulations incorporating thermal fluctuations showed no change in the observed exponents [12]. Further investigation would be of interest.

This work was supported by grants from the EPSRC and the European Community, and by a Sabbatical leave from Penn State University (J. R. B.).

*Permanent address: Department of Physics and Center for Materials Physics, The Pennsylvania State University, University Park, PA 16802.

[1] A. J. Bray, Adv. Phys. **43**, 357 (1994); H. Furukawa, Phys. Rev. A **31**, 1103 (1985).
[2] H. Furukawa, Physica (Amsterdam) **204A**, 237 (1994).
[3] F. Corberi, A. Coniglio, and M. Zannetti (to be published).
[4] E. Velasco and S. Toxvaerd, Phys. Rev. Lett. **71**, 388 (1993); J. Phys. Condens. Matter **6**, A205 (1994).
[5] P. Ossadnik, M. F. Gyure, H. E. Stanley, and S. C. Glotzer, Phys. Rev. Lett. **72**, 2498 (1994).
[6] R. Yamamoto and K. Nakanishi, Phys. Rev. B **49**, 14 958 (1994).
[7] G. Leptoukh, B. Strickland, and C. Rowland, Phys. Rev. Lett. **74**, 3636 (1995).
[8] J. E. Farrell and O. T. Valls, Phys. Rev. B **40**, 7027 (1989); **42**, 2353 (1990).
[9] J. E. Farrell and O. T. Valls, Phys. Rev. B **43**, 630 (1991).
[10] Y. Wu, F. J. Alexander, T. Lookman, and S. Chen, Phys. Rev. Lett. **74**, 3852 (1995).
[11] F. J. Alexander, S. Chen, and D. W. Grunau, Phys. Rev. B **48**, R634 (1993).
[12] S. Chen and T. Lookman (to be published).
[13] A. K. Gunstensen, D. H. Rothman, S. Zaleski, and G. Zannetti, Phys. Rev. A **43**, 4320 (1991).
[14] M. R. Swift, W. R. Osborn, and J. M. Yeomans, Phys. Rev. Lett. **75**, 830 (1995).
[15] E. Orlandini, M. R. Swift, and J. M. Yeomans, Europhys. Lett. (to be published).
[16] P. L. Bhatnagar, E. P. Gross, and M. Krook, Phys. Rev. **94**, 511 (1954); H. Chen, S. Chen, and W. H. Matthaeus, Phys. Rev. A **45**, R5339 (1992).
[17] J. S. Rowlinson and B. Widom, *Molecular Theory of Capillarity* (Clarendon Press, Oxford, 1982).
[18] W-J. Ma, P. Keblinski, A. Maritan, J. Koplik, and J. R. Banavar, Phys. Rev. Lett. **71**, 3465 (1993); see also S. E. May and J. V. Maher, Phys. Rev. Lett. **67**, 2013 (1991).